Proceedings of the Canadian Society for Mechanical Engineering International Congress
33rd Annual Conference of the Computational Fluid Dynamics Society of Canada
Canadian Society of Rheology Symposium
CSME-CFDSC-CSR 2026
May 24–27, 2026, Vancouver, British Columbia, Canada

Techno-economic parametric study of a low-temperature district heating network coupled with underground mine thermal energy storage

Frédéric Ransy[1,2], Aitor Cendoya[1], Pierre-Henri Gresse[3],Vincent Lemort[1]
[1]Aeropspace and Mechanical engineering, University of Liege, Liege, Belgium
[2]Wingest, Bastogne, Belgium
[3]Flexide Energy, Liège, Belgium

Abstract— This study presents a techno-economic analysis of a low-temperature district heating system coupled with underground mine thermal energy storage (UTES) in Martelange, Belgium. The system integrates photovoltaic panels, a geothermal heat pump, and a large water-filled mine reservoir to store seasonal thermal energy. Dynamic simulations in Modelica evaluate the impact of storage volume, storage cost, PV capacity, and battery size on key performance indicators such as COP, seasonal COP, self-consumption, self-sufficiency, storage efficiency, and cost of energy (COE). Results show that larger storage volumes increase renewable energy self-consumption but reduce seasonal performance due to higher thermal losses. Economically, storage investment cost dominates COE, while increasing PV or battery capacity improves self-sufficiency but does not always reduce costs. The analysis highlights a trade-off between flexibility, energy autonomy, and cost, demonstrating that intermediate storage sizes with moderate investment achieve the optimal balance for efficient and economically viable renewable heating systems.

Keywords: UTES, Slate Mine, district heating, energy efficiency, techno-economic analysis

I. INTRODUCTION

In order to reach climate neutrality by 2050, the European Union has developed a long-term strategy to progressively decrease greenhouse gas emissions [1]. Two dates are defined. First, a net emissions reduction by at least 55 % by 2030 compared to 1990 is desired. Second, a 2040 climate target of reducing by 90 % net greenhouse gas emissions, still relative to 1990 [1]. The strategy incorporates the deployment of renewable energy sources to replace fossil fuels and improvements in energy efficiency. The objectives, defined in the revised Renewable Energy Directive in [2], consider a minimum of 42.5 % of renewable energy production share, and 11.7 % reduction of EU final energy consumption by 2030.

The European Commission also defined a strategy in [3] to decarbonize the building sector. In fact, buildings represent a non-negligible source of CO_2 emissions in the EU, with about 40 % of energy consumption and 36 % of CO_2 emissions. The strategy focuses on the acceleration of the renovation rate of buildings and on the installation of low-carbon heating and cooling systems.

The installation of electric heat pump systems is an efficient way to decarbonize heating systems [4]. However, the electrification of the building sector, associated with the integration of intermittent renewable energy sources, makes electric grid operation more challenging, with potential problems of grid stability, flexibility, and security of supply [5].

The WeForming Horizon Europe project [6] addresses these challenges by developing and demonstrating technologies able to actively interact with the grid. The Belgian demonstrator in Martelange proposes a residential eco-district comprising several controllable assets to provide flexibility [7].

The innovation in the demonstrator is the combination of district heating with a large-scale mine underground thermal energy storage (MTES) and heat pump to increase self-consumption and self-sufficiency ratios, to provide flexibility, and shift energy demand to dynamically respond to grid signals. The project includes advanced control algorithms through digital twins to optimize energy flows.

The use of fourth generation heating networks allows the integration of different renewable energy sources (RES), such as waste heat, mine geothermal energy, heat generated by heat pumps, photovoltaic and solar thermal energy. Moreover, it can be combined with large-scale underground mine thermal energy storage to manage the intermittent and seasonal production of RES [8].

The mine thermal energy storage consists of abandoned water-filled mines repurposed as thermal storage. This concept has been already studied in Nova Scotia in Canada [9], in the Netherlands with the Heerlen Minewater Project [10], in Germany with the HT-MTES project [11], and in the United Kingdom [12]. This system has great potential for renewable energy integration and decarbonation of heating. However, the system can potentially face issues such as thermal short-circuiting due to direct hydraulic connection between hot and cold production wells, water quality, and long-term performance degradation. Other real case studies demonstrators are therefore necessary to validate the performance.

This paper presents the techno-economic analysis of a real case study of a mine thermal energy storage connected to a low-temperature district heating situated in Martelange, Belgium.

The project is part of the WeForming Horizon Europe project and is in the deployment phase. The paper focuses first on the case study description, then on the methodology and the models, and last the results are presented and discussed.

II. CASE STUDY DESCRIPTION

The demonstrator is located in the town of Martelange, in southwest Belgium. The site was previously utilized between 1895 and 1995 to extract blocks of shale to produce roofing slates. In the underground, the large number of extracted blocks created huge cavities from a depth of 40 to 160 meters. Fig. 1 shows the 3D representation of the underground cavities. In total, twelve chambers were created during the exploitation. They are divided into two categories of depth: between -40 and -120 meters from the surface, and from -120 and -160 meters. They are 10 meters wide, 30 meters deep, and vary in height between 60 and 80 meters. It represents about 300.000 m³ water-filled cavities. Unfortunately, certain cavities are also filled with shale waste resulting from exploitation in the 20th century, reducing the utilizable water volume.

Residential buildings are already integrated into the project, and will be connected in the near future to underground storage and district heating. Fig. 2 shows a top view of these buildings. In total, 60 apartment units spread over four buildings are constructed. Other constructions are also planned to reach the target of 150 apartment units in the district. The low-temperature district heating covers the heating demand.

The project includes several phases of development. The first phase consists of the design of the whole system. The second phase consists of the implementation of the underground storage and the heating of the underground water to reach the desired operating temperature. The third phase implies the construction of the district heating to provide heating to the building's occupants. The phase of design is completed and the implementation of the underground storage is in progress.

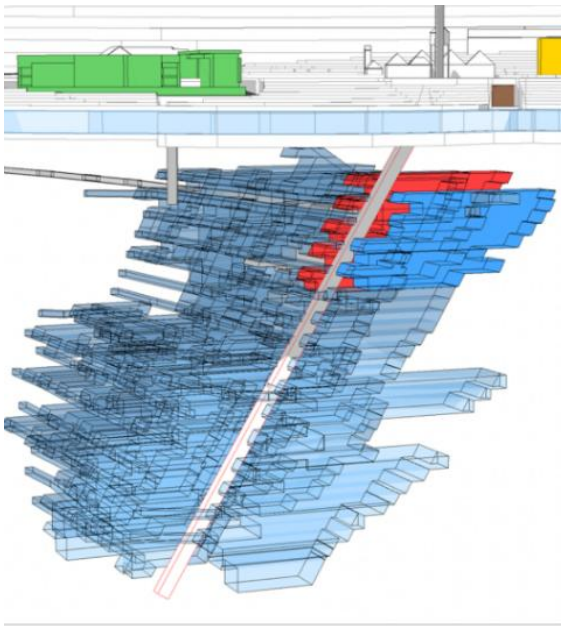

Figure 1: 3D representation of the underground cavities

Figure 2: Buildings integrated in the district

Figure 3: Underground storage components

Consequently, valuable information regarding investment costs is available and can be utilized to perform techno-economic parametric study, as proposed in this paper.

In order to provide heating to the building, the system comprises several assets: local renewable energy generation with photovoltaic panels, a geothermal heat pump, electric

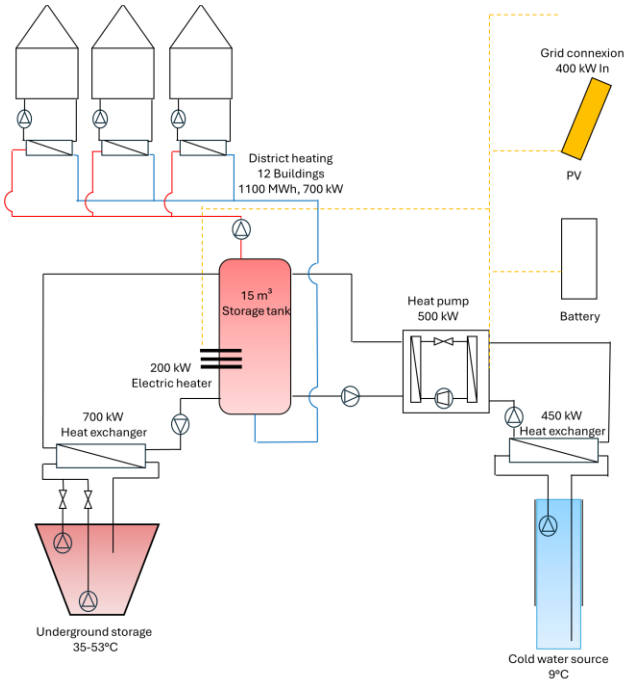

Figure 4: Hydraulic configuration in the project

resistance, chemical batteries, low-temperature district heating, a large underground mine thermal energy storage, several heat exchangers and pumps, a storage tank, and an advanced control algorithm through a digital twin.

The key asset in the system is the underground thermal energy storage. It consists of three vertical boreholes drilled to access each cavity. Each borehole contains a production well protected with steel casing along the entire height. The first well extracts hot water from the top, the second well cold water from the bottom, and the third well is the return line with hot or cold water, connected to a diffusion system. Fig. 3 shows underground storage components, with a borehole at the surface of the pipe, and the same pipe in the underground cavity.

The deployment of the system started with the closest cavity to the surface. The latest known plans indicated a 27000 m³ cavity. However, it turned out that 75 % of the volume was, in fact, occupied by shale waste fill. These measurements were conducted by divers over several dives. During the operation of the quarry, a large amount of waste was dumped into this cavity instead of being left on the surface due to a lack of space. As a result, the actual usable water volume is 6.500 m³, instead of the expected 27.200 m³.

However, this first deployment provided valuable information regarding the cost of the components of the storage system. This information can be utilized to correctly estimate the cost of the second cavity to be transformed into underground thermal energy storage. It is situated at a deeper depth (-120 to -180 meters), but with a known volume of 27.200 m³ totally filled only with water.

III. Methodology and Modeling

A. Model

The system presented in Fig. 4 is modeled in Modelica, an equation-based modeling language for complex physical systems. Several existing validated open-source libraries are utilized to model each component of the system. It allows accurate calculation of 15 min energy flows in the system, taking into account part load, and start-up and shutdown losses through dynamic simulations.

The buildings consist of 12 meters height apartment blocks containing 13 apartments over four floors, a basement garage and common areas, a total heated area of 1,401 m² and a volume of 3,447 m³. This geometry is utilized as a reference to determine the 15-minute timestep thermal power demand. The buildings built between 2019 and 2023 have excellent thermal insulation, high thermal inertia due to their concrete structure, and a single exhaust ventilation system combined with exhaust air heat pumps for individual domestic hot water production. Space heating is provided by underfloor heating regulated by individual room thermostats in each apartment. The reference building is modeled using the IDEAS (Integrated District Energy Assessment Simulations) library. This open-source library has been developed since 2013 by KU Leuven. It enables detailed modeling of buildings and heat production and distribution systems. The library, described in [13], has been validated as part of the IBPSA project 1 and the "Twin house IEA EBC Annex 58" case studies. The building envelope is described with detailed material properties to accurately represent thermal inertia and heat storage in the walls. The model divides the building into 15 thermal zones (13 apartments, a garage, and common areas), and takes into account convection, radiation, conduction, solar gains, and air infiltration. Each zone is connected to a ventilation system, an underfloor heating

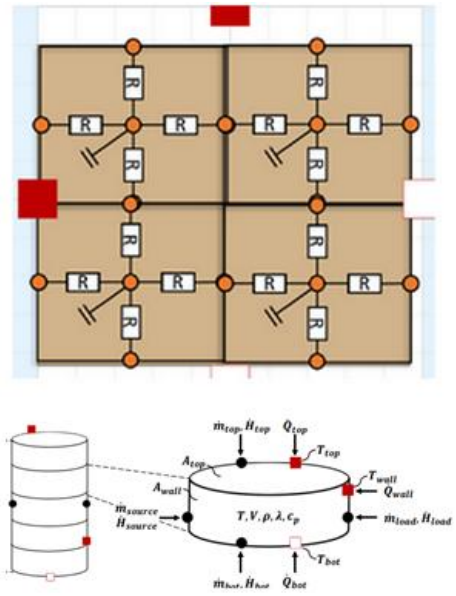

Figure 5: Underground storage modeling. R-C network (left). Water volume model (right).

system modeled according to EN 15337 [14] [15], and a thermostat to maintain indoor temperatures between 20 and 22°C. The other components of the system in Fig. 4 (heat exchangers, water tank, district heating, heat pump, circulation pumps) are also modeled with the IDEAS library. The heat pump model accounts for variations in COP and heating capacity with the condenser and evaporator temperatures, based on manufacturer data. Heat exchanger models include performance variations with inlet fluid temperatures and mass flow rates, with thermal inertia to accurately predict start-up evolutions. The water storage tank model considers water stratification through discretization into multiple volumes and heat losses to the environment. The pipes of the district heating are modeled using the IDEAS "plug-flow" approach in which the transport delay of temperature, pipe wall thermal inertia, heat losses along flow direction, and pressure drops are considered. The circulation pump consumption is calculated for each circuit with the pressure drop, the volumetric water flow rate, and the global efficiency, based on manufacturer data.

To model the electricity production of photovoltaic panels, the "photovoltaic-thermal collector" component of the IDEAS library is used. This model includes a module for electricity production. The model uses the "PVWatts v5 methodology" [16] and has been experimentally validated in [17]. The model parameters are the nominal power, the temperature coefficient, the surface area, and the nominal efficiency. The battery model consists of an energy balance to determine the state of charge, and a constant efficiency to take into account the losses.

The underground storage model uses the MoSDH library [18], by adapting an existing validated model. Fig. 5 shows the model, which has two components: the soil model, represented by an R-C network, and the water volume model, discretized into several layers. The R-C network allows the calculation of heat transfer and heat accumulation in the surrounding soil by taking into account thermal resistance and heat capacity. The stratification in the water reservoir is taken into account. The heat exchanges between the water, the surrounding soil, and the hydraulic system are calculated dynamically, to accurately reproduce the charging and discharging phases, and the thermal losses.

B. Performance indicators

In order to compare the simulation case studies, several key performance indicators are defined. They depend on the 15 min power values exchanged in the system: the thermal demand of the buildings $\dot{Q}_{buildings}$, the electrical power produced by the photovoltaic panels $\dot{W}_{PV}$, electrical power consumed by the system $\dot{W}_{load}$, the thermal power injected into and withdrawn from the Underground Thermal Energy Storage, $\dot{Q}_{sto,in}$ and $\dot{Q}_{sto,out}$, the thermal output power of the heat pump $\dot{Q}_{HP}$, and the electric input power of the heat pump $\dot{W}_{HP}$.

The electrical power produced by the photovoltaic panels is divided into two parts: the self-consumed part, denoted $\dot{W}_{PV,SC}$ and the part fed back into the electrical grid, These terms are calculated as follows:

$$\dot{W}_{PV,SC} = \min\left(\dot{W}_{PV}, \dot{W}_{load}\right) \quad (1)$$

$$\dot{W}_{PV,out} = \dot{W}_{PV} - \dot{W}_{PV,SC} \quad (2)$$

The electrical power consumed directly from the grid is denoted as $\dot{W}_{in,grid}$, and is calculated as follows:

$$\dot{W}_{in,grid} = \dot{W}_{load} - \dot{W}_{PV,SC} \quad (3)$$

The thermal and electrical power are then integrated over time to obtain the annual energy expressed in MWh. The following performance indicators are then defined:

$$COP = \frac{Q_{HP}}{W_{HP}} \quad (4)$$

$$SCOP = \frac{Q_{buildings}}{W_{load}} \quad (5)$$

$$SCR = \frac{W_{PV,SC}}{W_{PV}} . 100 \quad (6)$$

$$SSR = \frac{W_{PV,SC}}{W_{load}} . 100 \quad (7)$$

$$\varepsilon_{sto} = \frac{Q_{sto,out}}{Q_{sto,in}} \quad (8)$$

The COP of the heat pump is the ratio of the annual thermal energy produced by the heat pump to the heat pump's annual electricity consumption. The term SCOP represents the annual COP of the entire heat production system, calculated as the ratio of the annual energy supplied to the buildings, $Q_{buildings}$, to the total electricity consumption, W_{load} . The self-consumption ratio (SCR) represents the percentage of photovoltaic energy produced that is consumed directly on site. The self-sufficiency ratio (SSR) represents the percentage of the site consumption that is supplied directly by local photovoltaic energy. Ideally, a system based on renewable energy sources should approach self-consumption and self-sufficiency ratios of 100%. Finally, the term ε_{sto} represents the annual efficiency of underground thermal storage, calculated as the ratio of the energy extracted from storage ($Q_{sto,out}$) to the energy supplied to it ($Q_{sto,in}$).

The final performance indicator is the cost of energy supplied (COE), expressed in €/MWh. This is divided into two parts:

$$COE = CAPEX + OPEX \quad (9)$$

Where COE refers to the cost of energy, CAPEX refers to investment costs, and OPEX refers to costs related to operating the system. CAPEX costs are calculated with:

$$CAPEX = \frac{C_0\, \psi}{Q_{buildings}} \quad (10)$$

$$\psi = \frac{i}{1-(1+i)^{-N}} \quad (11)$$

Where C_0 is the initial investment cost for the complete system, ψ the annuity factor, i the interest rate fixed at 4 %, and N is the system's lifespan, considered to be 25 years. The batteries are considered to be replaced after 12.5 years. The estimated investment costs are as follows: 850 €/kWp for photovoltaic panels, 500 €/kWth for a heat pump, €40/kWe for an electrical resistor, 500 €/kWe for batteries, and 900,000 € for other components (piping, heat exchangers, circulation pumps, electrical cabinets, etc.). For underground storage, three values are considered: low price, 13 €/m³, medium price, 33 €/m³, and high price, 53 €/m³. These values are based on actual data from the WeForming project.

OPEX operating costs are calculated as follows:

$$OPEX = \frac{C_{el}+C_{O\&M}+C_{fixed}}{Q_{buildings}} \quad (12)$$

Where C_{el} denotes the total annual cost of electricity consumed from the grid (energy-based costs), $C_{O\&M}$ denotes the annual cost of operation and maintenance, and C_{fixed} are the fixed annual costs. The annual operation and maintenance costs are fixed at 1.5 % of the total capital cost. The fixed costs are 20.000 €/year for the DSO peak demand charges, and 20.000 €/year for the regional tax and the market operation costs. The energy-based costs are divided into two terms: the dynamic electricity price and the distribution and transmission network charges. Two electricity markets are considered: the 15 min Belgian day-ahead market and the 15 min balancing market. The heat pump is operated only on the day-ahead market, and the resistance can be activated on both the day-ahead and the balancing market, depending on the case study considered. The distribution and transmission network charges are imposed at 75 €/MWh. These values are based on real data from the WeForming project.

C. Design parameters and case studies considered

The system was designed to provide heat to about 150 apartment units, for a total of 1100 MWh of thermal energy, and 700 kW of peak thermal demand. The underground storage was designed, in consequence, with 700-kW nominal power heat exchanger connecting the underground water to the energy power plant. The operating temperature is varied between 35 and 53°C. The annual minimum value is imposed by the return temperature of the district heating, imposed by the emitters in the buildings (underfloor heating), and the maximum temperature is imposed by cooling limitations of the submersible pumps. Two production assets are combined to produce hot water: a 500 kW capacity geothermal heat pump and 200 kW electric resistance. The heat pump is fed into the evaporator with 9°C cold water from the mine. This design was selected to minimize the energy cost for the occupants, with a given maximum grid peak power of 400 kW. All the components are connected together through a 15 m³ storage tank located at the surface, allowing the energy to be exchanged between the production assets, the district heating and the underground storage. This component also provides thermal inertia to avoid frequent on-off heat pump activations. The system also includes PV panels and a chemical battery to maximize self-consumption.

The simulations consider two distinct phases. First, the underground water is heated with local renewable energy for 2 years and a half. In that phase, the buildings are disconnected. Second, the buildings are connected, the underground storage is activated, and the simulation is performed over one year, from the first of October.

In order to assess the impact on the performance indicators, several simulations are carried out with different case studies and system parameters. First, the reference case without the balancing market consists of the system presented in Fig. 4, but without the underground storage, and with only the day-ahead electricity market to activate the heat pump and the resistance. Second, the reference case with the balancing market also considers an absence of underground storage, but the electric resistance can be activated by the imbalance electricity market. Third, other cases are considered with three underground water volumes: 6.500 m³, 18.000 m³ and 27.000 m³. The photovoltaic panel peak power is also varied (200 kWp and 400 kWp), and the battery capacity is changed (60 kWh and 120 kWh).

IV. Results and Discussion

This section presents the results, divided into three sub-sections: the evolution of the temperature in the cavities, Sankey diagrams to visualize the energy flows, and a synthesis table to provide an overview of the simulation results.

Fig. 6 shows the evolution of the temperature of the underground water at the middle of the reservoir, for 6500 m³ (blue), 18000 m³ (orange) and 27000 m³ (gray). For both the simulations, the PV panels and battery designs are fixed to 200 kWc and 60 kWh, respectively. The storage temperature shows a seasonal trend, with a decrease from November to February, and an increase from March to June. The smallest volume (6500 m³) shows the largest annual temperature variation and the strongest short-term variations, with monthly-and day-to-day variations. In particular, an increase in the storage temperature is observed during January, followed by a significant decrease

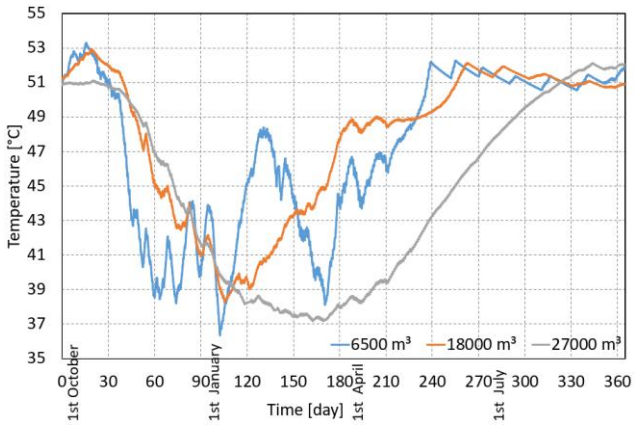

Figure 1: Evolution of temperature in the underground cavity, for 6500 m³, 18000 m³ and 27000 m³

in February and March. This behavior is driven by more favorable electricity price conditions on January, and less favorable conditions in February and March. In contrast, the temperature evolution in the largest reservoir (27000 m³) is smoother, with a gradual increase during the charging period and attenuated day-to-day variations. These results indicate an interconnection between the storage volume and the system operation strategy. The smallest volume enforces conservative operation with limited depth of discharge and stricter operational control to maintain acceptable temperature levels.

Fig. 7 represents three Sankey diagrams to visualize energy flows in the system for three case studies. It also illustrates different operational strategies for an energy system composed of PV generation, grid electricity, a heat pump, electric resistance heating, and underground thermal storage supplying building heating demand. In both cases, the PV peak power is 200 kWp, and the battery capacity is 60 kWh.

In case (a), the system is not connected to the underground storage, and the heat pump and resistance are activated on the day-ahead electricity market only. In that configuration, the heat pump provides the majority of thermal energy, and the grid's electric consumption remains moderate. However, a large proportion of PV production is exported to the grid because the thermal inertia in the system is not sufficient. This configuration prioritizes efficiency over flexibility.

In case (b), the underground storage is not considered yet, but the electric resistance heater can be activated for balancing services that can generate revenues. As a consequence, resistance heating and grid electricity consumption increase significantly, while the heat pump contribution decreases. The system shifts from an efficient-driven operation toward a market-driven flexibility strategy. Electricity is intentionally converted into heat with lower efficiency because the balancing market compensates for the additional consumption. However, a large amount of PV production is still exported to the grid.

In case (c), thermal energy storage is introduced to optimize electricity consumption on day-ahead and balancing markets. In this configuration, the thermal storage absorbs a large share of the heat production. It leads to thermal losses, but enables temporal shifting of consumption. Grid consumption increases again, and a lower amount of PV production is exported to the grid. This configuration is a flexible and multi-energy hub that prioritizes economic optimization and flexibility provision over pure energy efficiency.

Table 1 summarizes the parametric study conducted to evaluate the influence of photovoltaic (PV) capacity, battery size, and underground thermal storage volume and price on system performance and the resulting cost of energy (COE). Nineteen scenarios were simulated by varying PV installed power (200 and 400 kWp), battery capacity (60 and 120 kWh), seasonal thermal storage volume (from 0 to 27,000 m³), and storage investment costs (13 to 53 €/m³). For each configuration, key performance indicators were assessed, including the coefficient of performance (COP), seasonal coefficient of performance (SCOP), self-consumption ratio (SCR), self-sufficiency ratio (SSR), storage efficiency, and COE.

The results show that increasing the thermal storage volume significantly enhances renewable energy utilization. The SCR increases from 34% without storage to nearly 100% for the largest storage configurations, while SSR also improves, indicating greater local use of PV production. However, this increased autonomy is accompanied by a degradation of seasonal performance, as reflected by the decrease in SCOP from approximately 2.5 to values between 1.5 and 1.7 for large storage systems. This trend suggests higher thermal losses. This also indicates a higher energy consumption of the electric heater resistance on the balancing market.

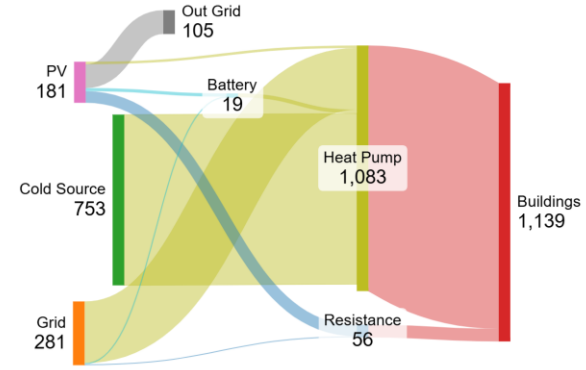

(a) Reference case without balancing market

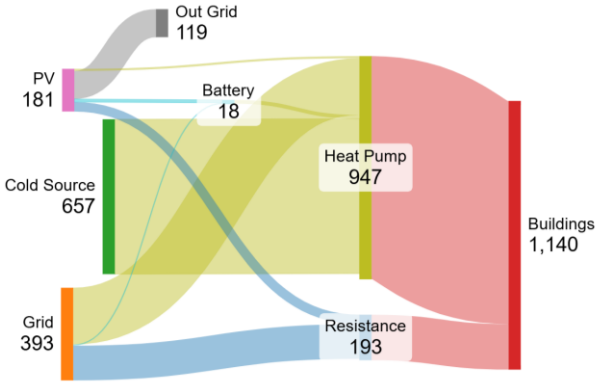

(b) Reference case with balancing market

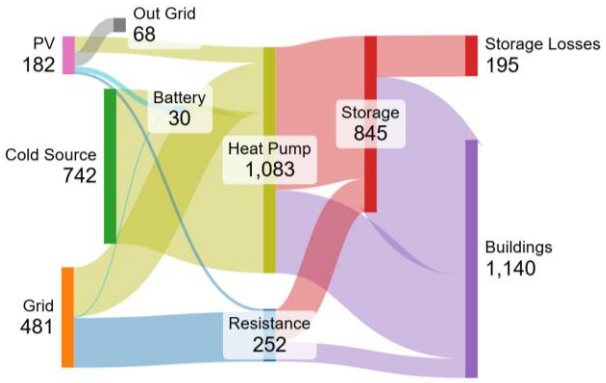

(c) Case with storage volume of 6500 m³

Figure 2: Sankey diagrams to visualize the annual energy flows for three case studies, expressed in kWh

Table 1: Summary of simulation results. The parameters for each of the simulations are listed on the left. The performance indicators defined previously are listed on the right. The first simulation is the reference case, without underground storage.

N°	Parameters				Values					
	P_{PV} [kWp]	C_{batt} [kWh]	Vol_{Sto} [m³]	*Price Sto [€/m³]*	*COP [-]*	*SCOP [-]*	*SCR [%]*	*SSR [-]*	ε_{sto} *[%]*	*COE [€/MWh]*
1	200	60	0	-	3.8	2.5	34	13	-	163
2	200	60	6500	13	3.7	1.9	63	19	77	159
3	200	60	6500	33	3.7	1.9	63	19	77	167
4	200	60	6500	53	3.7	1.9	63	19	77	176
5	400	120	6500	13	3.6	1.9	57	34	78	167
6	400	120	6500	33	3.6	1.9	57	34	78	176
7	400	120	6500	53	3.6	1.9	57	34	78	185
8	200	60	18000	13	3.6	1.7	75	20	66	169
9	200	60	18000	33	3.6	1.7	75	20	66	194
10	200	60	18000	53	3.6	1.7	75	20	66	218
11	400	120	18000	13	3.5	1.6	77	39	71	171
12	400	120	18000	13	3.5	1.6	77	39	71	196
13	400	120	18000	13	3.5	1.6	77	39	71	221
14	200	60	27000	13	3.6	1.5	100	24	65	165
15	200	60	27000	33	3.6	1.5	100	24	65	203
16	200	60	27000	53	3.6	1.5	100	24	65	240
17	400	120	27000	13	3.5	1.5	97	45	65	171
18	400	120	27000	33	3.5	1.5	97	45	65	209
19	400	120	27000	53	3.5	1.5	97	45	65	247

Storage efficiency also decreases with increasing volume. From an economic perspective, the investment cost of the storage system plays a dominant role. For identical technical performance, COE increases with storage cost, demonstrating that capital expenditures outweigh operational benefits once a sufficient level of flexibility is achieved. While increasing PV capacity and battery size improve self-sufficiency, it does not systematically reduce COE, as higher investment costs and periods of surplus production limit additional economic gains. Overall, the results highlight a trade-off between energy autonomy and economic performance. Thermal storage primarily acts as a flexibility solution that enhances renewable integration rather than as a direct cost-reduction technology. The lowest COE values are obtained for intermediate storage sizes combined with low investment costs, indicating that optimal system design requires techno-economic balancing rather than maximizing storage capacity or renewable penetration.

V. Conclusion

The techno-economic analysis of the Martelange demonstrator highlights the potential and limitations of coupling low-temperature district heating with large-scale underground mine thermal storage. The simulations show that seasonal thermal storage can significantly increase self-consumption of locally generated renewable energy, providing temporal flexibility and enabling interaction with electricity markets. However, larger storage volumes result in higher thermal losses, lower seasonal COP, and increased reliance on electric resistance heating, illustrating a trade-off between energy autonomy and system efficiency. The use of electric resistance results from participation in electricity markets (flexibility), enabled by the use of the underground thermal energy storage. From an economic perspective, storage investment cost is the primary driver of the cost of energy, while increasing PV capacity or battery size enhances self-sufficiency but offers limited COE reduction. The optimal system design requires a techno-economic balance: intermediate storage sizes combined with optimized local renewable energy production through photovoltaic provide the best compromise between flexibility, renewable energy utilization, and economic performance. These findings support the deployment of UTES-based district heating as a flexible solution for decarbonizing residential heating while integrating renewable energy sources efficiently.

Acknowledgment

The authors would like to acknowledge the funding provided by the European Union's Horizon Research and Innovation program under grant agreement No. 10112355, in the framework of the WeForming project. The authors would also like to acknowledge the funding provided by the Walloon Region of Belgium in the framework of the ARDNrgy project.

REFERENCES

[1] European Commission. (2025). *2040 EU climate target: A path to competitiveness & climate neutrality by 2050* (Report). Directorate-General for Climate Action. https://op.europa.eu/en/publication-detail/-/publication/c2cbd98c-5881-11f0-a9d0-01aa75ed71a1/language-en

[2] European Union. (2023). *Directive (EU) 2023/2413 of the European Parliament and of the Council of 18 October 2023 amending Directive (EU) 2018/2001, Regulation (EU) 2018/1999 and Directive 98/70/EC as regards the promotion of energy from renewable sources, and repealing Council Directive (EU) 2015/652* (Renewable Energy Directive RED III). *Official Journal of the European Union, L 2413.* https://eur-lex.europa.eu/eli/dir/2023/2413/oj

[3] European Commission. (2020). *A Renovation Wave for Europe – greening our buildings, creating jobs, improving lives* (COM(2020) 662 final). Brussels: European Commission. Disponible sur https://eur-lex.europa.eu/legal-content/EN/ALL/?uri=CELEX%3A52020DC0662

[4] Thomaßen G., Kavvadias K., Jiménez Navarro J. P. (2021). *The decarbonisation of the EU heating sector through electrification: A Parametric analysis*, Energy Policy, Volume 148, Part A,n111929, ISSN 0301-4215, https://doi.org/10.1016/j.enpol.2020.111929.

[5] Khalid, M. (2024). Smart grids and renewable energy systems: Perspectives and grid integration challenges. *Energy Strategy Reviews*. https://doi.org/10.1016/j.esr.2024.101299.

[6] *European Commission.* (2026). Buildings as Efficient Interoperable Formers of Clean Energy Ecosystems (Grant Agreement No. 101123556). CORDIS. https://doi.org/10.3030/101123556

[7] Cendoya, Aitor & Ransy, Frédéric & Lemort, Vincent & Hernandez, Andres & Dewallef, Pierre & Gresse, Pierre-Henri & Windeshausen, Jacques. (2024). Modelling and Simulation of a Carnot Battery Coupled to Seasonal Underground Stratified Thermal Energy Storage for Heating, Cooling and Electricity Generation. Proceedings of the 8th International High Performance Buildings Conference at Purdue, July 15 – 18, 2024.

[8] Guelpa, E., & Verda, V. (2019). Thermal energy storage in district heating and cooling systems: A review. *Applied Energy*, 252, 113474.

[9] Sohrabikhah, S., & Hughes, L. (2025). A Performance Evaluation and Feasibility Study of Mine Thermal Energy Storage in Glace Bay, Nova Scotia. *Energies*, *18*(17), 4780. https://doi.org/10.3390/en18174780

[10] Verhoeven, R.; Willems, E.; Harcouët-Menou, V.; Boever, E.D.; Hiddes, L.; Veld, P.O.; Demollin, E. Minewater 2.0 project in Heerlen the Netherlands: Transformation of a geothermal mine water pilot project into a full scale hybrid sustainable energy infrastructure for heating and cooling. In Proceedings of the 8th International Renewable Energy Storage Conference and Exhibition, IRES 2013, Berlin, Germany, 18–20 November 2013.

[11] Hahn, F.; Jagert, F.; Bussmann, G.; Nardini, I.; Bracke, R.; Seidel, T.; König, T. The reuse of the former Markgraf II colliery as a mine thermal energy storage. In Proceedings of the European Geothermal Congress 2019, Den Haag, The Netherlands, 11–14 June 2019

[12] Banks, D.; Athresh, A.; Al-Habaibeh, A.; Burnside, N. Water from abandoned mines as a heat source: Practical experiences of open- and closed-loop strategies, United Kingdom. *Sustain. Water Resour. Manag.* 2019, *5*, 29–50

[13] F. Jorissen, G. Reynders, R. Baetens, D. Picard, D. Saelens, and L. Helsen, "Implementation and verification of the IDEAS building energy simulation library", Journal of Building Performance Simulation, vol. 11, no. 6, pp. 669–688, 2018.

[14] EN 15377, Heating systems in buildings – Design of embedded water-based surface heating and cooling systems., 2008.

[15] M. Koschenz and B. Lehmann, Thermoaktive Bauteilsysteme tabs. Dübendorf, Switzerland: EMPA Energyiesysteme/Haustechnik, 2000, ISBN: 9783905594195.

[16] Dobos, A. P. (2014). PVWatts Version 5 Manual. NREL/TP-6A20-62641

[17] Meertens, L., Jansen, J., Helsen, L. (2025). Development and Experimental Validation of an Unglazed Photovoltaic-Thermal Collector Modelica Model that only needs Datasheet Parameters, submitted to the 16th International Modelica & FMI Conference, Lucerne, Switzerland, Sep 8–10, 2025

[18] J. Formhals "Object-oriented modeling of solar district heating systems with underground thermal energy storage," Dissertation, Technical University of Darmstadt, 2022.